Quantitative and structural analysis of water association in water-lithium bromide-1,3-dimethylimidazolium chloride mixtures

David Latorre-Arca [a,e], M. Soledad Larrechi [b,e,*], Daniel Salavera [a,e], Alberto Coronas [a,e], Antonio Rodríguez-Fortea [c,*], Alejandro Rivera-Pousa [d], Trinidad Méndez-Morales [d,*], Luis M. Varela [d]

[a] *Mechanical Engineering Dept, Universitat Rovira i Virgili, Tarragona, Spain*
[b] *Analytical and Organic Chemistry Dept, Universitat Rovira i Virgili, Tarragona, Spain*
[c] *Quantum Chemistry Group-QCG, Physical and Inorganic Chemistry Dept, Universitat Rovira i Virgili, Tarragona, Spain*
[d] *Nanomaterials, Photonics and Soft Matter Group-NaFoMat, Particle Physics Dept, Universidade de Santiago de Compostela, Santiago de Compostela, Spain*
[e] *Group of Research in Applied Thermal Engineering-CREVER, Mechanical Engineering Dept, Spain*

* Corresponding authors.
E-mail addresses: mariasoledad.larrechi@urv.cat (M. Soledad Larrechi), antonio.rodriguezf@urv.cat (A. Rodríguez-Fortea), trinidad.mendez@usc.es (T. Méndez-Morales).

1. Introduction

Absorption refrigeration systems are an alternative to conventional vapor-compression systems because they are activated by heat energy sources and can use natural refrigerants as working fluids. Since the middle of the 20th century, the mixture of water + lithium bromide (H_2O+LiBr) has been widely used as a working fluid in this technology, due to the special properties of water as the refrigerant and lithium bromide as absorbent. However, the risk of crystallization of the salt at low temperatures is an important inconvenience and a limitation of this type of technology.

Ionic liquids (ILs), characterized by negligible vapor pressure and strong water absorption capacity, have been recently proposed as suitable additives of (H_2O+LiBr) to overcome the abovementioned limitation [1–5].

Knowing the effects of ILs on the physicochemical properties of the mixture is of crucial importance to select them and evaluate their suitability as additives in the conventional working fluids. For this purpose, it is relevant to evaluate and understand how the solvation of lithium and bromide ions changes when the IL is added.

In the literature, methods based on: ^{1}H -NMR [6–8], FTIR [9,10], neutron diffraction [11–13] are usually referenced to study the solvation structures of inorganic salts and IL ions in water.

NIR spectroscopy along with a curve resolution method based on alternating least squares (MCR-ALS) [14] has been used to elucidate the association of imidazolium-

based ILs in water [15,16]. The authors have used this methodology to determine quantitatively the amount of free water in aqueous mixtures of lithium salts [17] and ILs based on the imidazolium cation [18].

The main objective of this work consists in extracting information about the role of 1,3-dimethylimidazolium chloride ([Dmim][Cl]) in the solvation process of the ions when it is added to the working pair (H_2O+LiBr). This IL, which has been referenced as a good additive [2], is used to study quantitatively and structurally the water association in (H_2O+LiBr+[Dmim][Cl]) mixtures.

The soft modeling resolution curve method based on alternating least squares (MCR-ALS) has been applied to the near-infrared (NIR) spectra of (H_2O+LiBr+[Dmim][Cl]) mixtures prepared with an absorbent (LiBr+[Dmim][Cl]) mole fraction ranging from 0 to 0.5987 (0.2944 + 0.3043).

In addition, to compare the absorption ability of the ternary mixture with that of the conventional (H_2O+LiBr), a quantitative analysis of the association of water in aqueous mixtures with LiBr (mole fraction from 0 to 0.2026) and with [Dmim][Cl] (mole fraction from 0 to 0.1426) has also been done.

The (NIR+MCR-ALS) methodology is used to: a) determine the amount of free water in the mixtures and analyze the effect of the IL in the water association, and b) estimate the mol ratio (n) among H_2O/absorbent of the solvated structures formed in the different mixtures. The result for the ternary mixtures (H_2O+LiBr+[Dmim][Cl]) are compared with the results of the computational study performed to analyze the structure and arrangement of water molecules.

Thus, to complement the experimental results and shed some light on the molecular environment in the solvation shells around the ions in water, we have also performed molecular dynamics (MD) simulations of the abovementioned ternary mixtures for different concentrations (see 2.4 Computational details). Both computational and experimental methods are employed to fully characterize the ternary (H_2O+LiBr+[Dmim][Cl]) solutions.

Although some computational studies analyzing the solvation process and the structural properties of inorganic salts mixed with ILs have been previously reported [19,20], the number of articles concerning ternary mixtures is very limited and they mainly focus on the addition of carbonates or dimethyl sulfoxide to ILs+inorganic salts [21] for electrochemical applications. Thus, to the best of our knowledge, there exists no

work that has explored ternary mixtures involving ILs, water, and alkali metal salts using molecular simulations.

2. Experimental section

2.1 Water-mixtures

Water binary mixtures of lithium bromide (H_2O+LiBr) and 1,3-dimethylimidazolium choride (H_2O+[Dmim][Cl]) and ternary mixtures of (H_2O+LiBr+[Dmim][Cl]) were prepared using the reagents supplied by Honeywell Fluka (LiBr, purity 99%) and Angene ([Dmim][Cl], purity > 97%) and Millipore water ($\rho <$ 18.2 MΩ cm). Before its use, the lithium bromide was heated and dried at 353.15 K in an oven. The IL was heated and stirred at 333.15 K under vacuum conditions ($3x10^{-2}$ mbar) for 48 h, to remove traces of water. For each mixture, twelve solutions were prepared by weight using an analytical balance (Mettler Delta Range, mod. AE260). Table 1 shows the masses used to prepare binary and ternary mixtures and the LiBr and/or [Dmim][Cl] mole fraction.

Table 1. Amount of H_2O, LiBr and [Dmim][Cl] used to prepare the binary and ternary mixtures and their respective mole fraction of LiBr and [Dmim][Cl] in the mixtures.

a) (H_2O+LiBr)			*b*) (H_2O+[Dmim][Cl])			*c*) (H_2O+LiBr+[Dmim][Cl])				
m_{H2O} (g)	m_{LiBr} (g)	x_{LiBr}	m_{H2O} (g)	$m_{[Dmim][Cl]}$ (g)	$x_{[Dmim][Cl]}$	m_{H2O} (g)	m_{LiBr} (g)	$m_{[Dmim][Cl]}$ (g)	x_{LiBr}	$x_{[Dmim][Cl]}$
5.3194	0	0	4.9582	0	0	5.1376	0	0	0	0
5.1682	0.2722	0.0108	4.7834	0.2517	0.0071	4.9049	2.8398	0.4078	0.1062	0.0100
3.9101	0.4322	0.0224	3.8527	0.4285	0.0149	4.6260	2.9876	0.8361	0.1156	0.0212
4.3068	0.7585	0.0352	4.6542	0.8188	0.0233	4.8247	3.3902	1.4258	0.1229	0.0339
4.2382	1.0578	0.0492	3.8824	0.9717	0.0329	4.5501	3.5773	2.0490	0.1332	0.0500
3.9855	1.3278	0.0646	4.2415	1.4165	0.0434	3.7824	3.2865	2.3565	0.1425	0.0669
3.9353	1.6876	0.0817	4.1601	1.7825	0.0550	2.9127	2.9257	2.5203	0.1571	0.0887
5.2366	2.8387	0.1011	3.4481	1.8559	0.0681	2.9161	3.3934	3.3799	0.1726	0.1126
6.8127	4.5407	0.1215	3.3485	2.2303	0.0830	2.0188	2.8402	3.2263	0.1934	0.1439
5.9973	4.9212	0.1455	3.0089	2.4602	0.1000	1.8078	3.1364	4.0516	0.2162	0.1830
6.4967	6.4979	0.1718	2.8244	2.8189	0.1194	1.3597	3.2038	4.5424	0.2516	0.2336
5.9397	7.2762	0.2026	2.6705	3.2691	0.1426	0.8810	3.1166	4.9185	0.2944	0.3043

u(m) = 0.0002 g

2.2 Near-Infrared measurements

The near-infrared spectrum of each mixture was obtained between 900 nm and 1060 nm using an Ocean Optics UV-Vis-NIR (Maya 2000 pro) spectrophotometer equipped with optical fibers. The spectra data vector contains 380 absorbance values at intervals of 0.4215 nm. A standard quartz cuvette with a 1 cm optical path was used for the measurements. The 100% of transmittance was established in the spectrophotometer using the empty cuvette. The cuvette was filled with an aliquot of each mixture to acquire its individual spectra. To control the temperature, the closed cuvette and the mixtures were heated in a thermostatic water bath in which the temperature was controlled with a thermometer, and the cuvette was filled with each mixture into the bath before measuring. The different mixtures were sequentially measured.

2.3 Data analysis details

The spectra obtained for the ternary and binary mixtures were arranged in individual data matrices; $\mathbf{M}_{H2O+LiBr+[Dmim][Cl]}$, $\mathbf{M}_{H2O+LiBr}$, and $\mathbf{M}_{H2O+[Dmim][Cl]}$ of dimensions *(12 x 380)*. The matrices were processed in MATLAB (The MathWorks INC., Natick, Ma, v 2018). In each matrix, the spectra were preprocessed using a weighted-least-squares baseline function of PLs-Toolbox v7 (the Eigenvector Research, Manson, WA) to eliminate the baseline shift.

To quantify the interaction between the water molecules and the ions, the multivariate curve resolution method based on alternating least squares (MCR-ALS) was applied to the individual spectra data matrix, in general $\mathbf{M_i}$ of dimensions *(12 x380),* using the toolbox developed by Jaumot et al. [14]. Assuming a bilinear model, this method decomposes the data matrix $\mathbf{M_i}$ into the product of two matrices according to the equation $\mathbf{M_i} = \mathbf{C_i S_i^T} + \mathbf{E_i}$. The $\mathbf{C_i}$ matrix of dimensions *(12 x n)* contains the concentration profiles of the *n* components in the analyzed solutions and the $\mathbf{S_i^T}$ matrix of dimensions *(n x 380)* contains their related pure spectra. The $\mathbf{E_i}$ matrix of dimensions *(12 x 380)* contains information unexplained by the resolution model.

MCR-ALS involves several stages. First, the number of components in the solution (*n* value) must be selected. In our work, this number represents the different chemical environments in which there is water, either as bulk water or associated with LiBr and/or [Dmim][Cl]. This number was determined by examining the explained

variance percentage of the singular values calculated by singular value decomposition (SVD) [22] of each spectral data matrix $\mathbf{M_i}$. Second, an initial estimate of $\mathbf{S_i^T}$ or $\mathbf{C_i}$ is required before initializing the optimization step. In this work, the algorithm was initialized using the initial estimation of the $\mathbf{C_i}$ matrix, obtained from evolving factor analysis (EFA) [23]. This estimate is iteratively optimized by a constrained alternating least squares (ALS) regression procedure. The used restrictions, were non-negativity of spectra and concentration profiles, unimodality of concentration profiles, and normalization of the spectra. A convergence criterion value of 0.01 was considered.

The quality of MCR-ALS solutions is evaluated using the lack of fit (LOF) and explained variance (R^2) parameters, which identify the dissimilarity between the experimental spectra data matrix ($\mathbf{M_i}$) and the data reproduced ($\mathbf{C_iS_i^T}$) by MCR-ALS. The closer the values of LOF and R^2 are to zero and one, respectively, the better the fit of the experimental data. In this work, the similarity coefficient (r) between the spectrum of pure water and the spectrum recovered by MCR-ALS as representative of bulk water in the solutions has also been calculated to evaluate the goodness of the resolution.

2.4 Computational details

To obtain a detailed picture at a molecular level of the solvation structure of the ions in water, atomistic MD simulations of ternary mixtures of (H_2O+LiBr+[Dmim][Cl]) were performed using the GROMACS 2020.4 package [24,25] with the non-polarizable OPLS-AA force field [26]. The parameters for lithium and bromide are those provided by the force-field (opls_404 and opls_402, respectively), whereas those for chloride were obtained from Ref. [27]. In these simulations, the parameterization employed for the imidazolium cation was constructed by Canongia Lopes *et al.* [28] whereas the five-site TIP5P model of Mahoney and Jorgensen [29] was used for water.

Five different concentrations were chosen from Table 1.c with the aim of covering the whole experimental range with computational calculations. For each simulation, the total number of molecules was set to 5000 and the number of molecules of each type is specified in Table 2.

Table 2. Number of molecules of each type for the different concentrations studied with MD simulations.

x_{LiBr}	$x_{[Dmim][Cl]}$	N_{LiBr}	$N_{[Dmim][Cl]}$	N_{H2O}
0.1062	0.0100	531	50	4419
0.1229	0.0339	614	170	4216
0.1571	0.0887	785	444	3771
0.1934	0.1439	967	720	3313
0.2944	0.3043	1472	1522	2006

In addition, a simulation of pure water with 1000 molecules was carried out with the purpose of comparison, and the results are included in the supplementary information S1. The PACKMOL software [30] was employed to obtain the initial configurations in which the molecules were randomly distributed inside a cubic simulation box. Then, the energy of these artificially generated configurations was minimized using the steepest descent algorithm [31], with a maximum step size and tolerance set to 0.01 nm and 0.1 kJ/(nm·mol), respectively. This was followed by a stabilization run of 25 ns with a time step of 1 fs in the isothermal-isobaric (NpT) ensemble to reach the experimental density at T = 298.15 K (using the V-rescale thermostat [32]) and p = 1 atm (set by a Parrinello-Rahman barostat [33]). Then, a new stabilization run of 10 ns in the NVT ensemble was performed. The resulting stable configuration is employed as input for a production run of 10 ns, in which the atomic positions were recorded every 5 ps and used for the structural analysis. Additionally, short simulations of 100 ps were performed recording the velocity of each atom in all the simulation frames to compute the vibrational density of states (vDos). Periodic boundary conditions were applied in all directions and Coulomb interactions were treated by using the Particle Mesh Ewald (PME) method [34] with a grid spacing of 12 nm and cubic interpolation. A cut-off radius of 1.1 nm was used for both short and long-range interactions. The Linear Constraint Solver (LINCS) algorithm [35], with a fourth order expansion of the constraint coupling matrix, was used to fix all the bond lengths with H atoms.

Car-Parrinello molecular dynamics simulations were carried out using the CPMD code [36,37]. The description of the electronic structure was based on the expansion of the valence electronic wave functions into a plane wave basis set, which was limited by

an energy cutoff of 70 Ry. The interaction between the valence electrons and the ionic cores was treated through the pseudopotential (PP) approximation (Martins−Troullier type) [38]. The PBE density functional was selected [39]. The simulations were carried out under periodic boundary conditions in a cubic cell with a side length that slightly depends on the system (see below), a fictitious electron mass of 1300 a.u. and a time step of 0.144 fs. Car-Parrinello MD simulations were done for two different (H_2O+LiBr+[Dmim][Cl]) mixtures, (i) mole fraction $x_{[Dmim][Cl]} = 0.0357$, that is, 48 H_2O + 6 LiBr + 2 [Dmim][Cl] and side length of 12.590 Å; and (ii) mole fraction $x_{[Dmim][Cl]} = 0.3000$, that is, 8 H_2O + 6 LiBr + 6 [Dmim][Cl] and side length 12.000 Å. The systems were initialized and then equilibrated for 28 ps at the simulated temperature 300 K. The production runs were 60 ps long. To analyze the spatial correlations of the different species in the mixtures we have calculated their radial distribution functions (RDFs) and their integrations, i.e. the coordination numbers.

3. Results and discussion

3.1 Infrared analysis and MCR-ALS resolution

Figure 1 shows the pre-treated NIR spectra of the (H_2O+LiBr+[Dmim][Cl]) prepared mixtures. The absorption band around 973 nm, which is characteristic of the stretching vibration of the –OH group, decreases with water concentration in the mixtures, and the peak is displaced towards longer wavelengths. This behavior can be attributed to the formation of different solvated structures due to the interaction between water molecules and ions through hydrogen bonds [7,9,15,40,41]. In addition, it is possible to see an intensity increase in the spectral region between 900 nm and 920 nm, which is characteristic of the stretching vibration of the –CH group present in the IL [42].

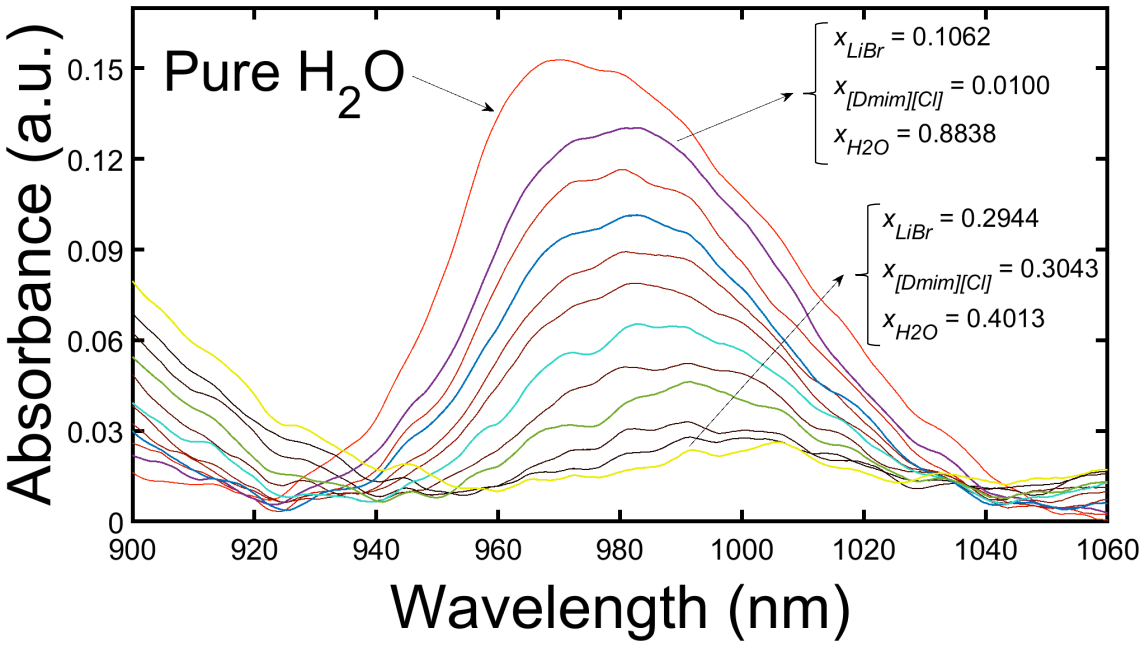

Figure 1. Pre-treated NIR spectra of the (H_2O+LiBr+[Dmim][Cl]) ternary mixtures.

The spectral trend is similar to the one discussed by the authors in their previous works, in which the amount of water not involved in the solvation of LiBr [17] or the [Dmim][Cl] [18] was quantitatively determined from MCR-ALS analysis of NIR spectra of aqueous solutions, measured at different temperatures as the one considered in the present work (T = 25 ºC). The spectra of binary mixtures, obtained to analyze comparatively the water association in ternary mixtures (H_2O+LiBr+[Dmim][Cl]) with respect to the binary (H_2O+LiBr) or (H_2O+[Dmim][Cl]) ones, are included in supplementary information S2.

The joint spectroscopy analysis of the binary and ternary mixtures spectra does not allow us to evaluate whether the behavior of the spectra in the ternary mixtures agrees or not with the expected considering the simultaneous contribution of each component (LiBr+[Dmim][Cl]). To facilitate the discussion, in Figure 2 we have included, along with the water spectrum, one spectrum of each mixture with a relatively similar absorbent mole fraction. The spectra A and B are the spectrum of binary lithium bromide (x_{LiBr} = 0.1215) and IL ($x_{[Dmim][Cl]}$=0.1194) mixed with water, respectively, and the spectrum C (x_{LiBr} = 0.1062 + $x_{[Dmim][Cl]}$ = 0.0100) corresponds to the ternary mixtures.

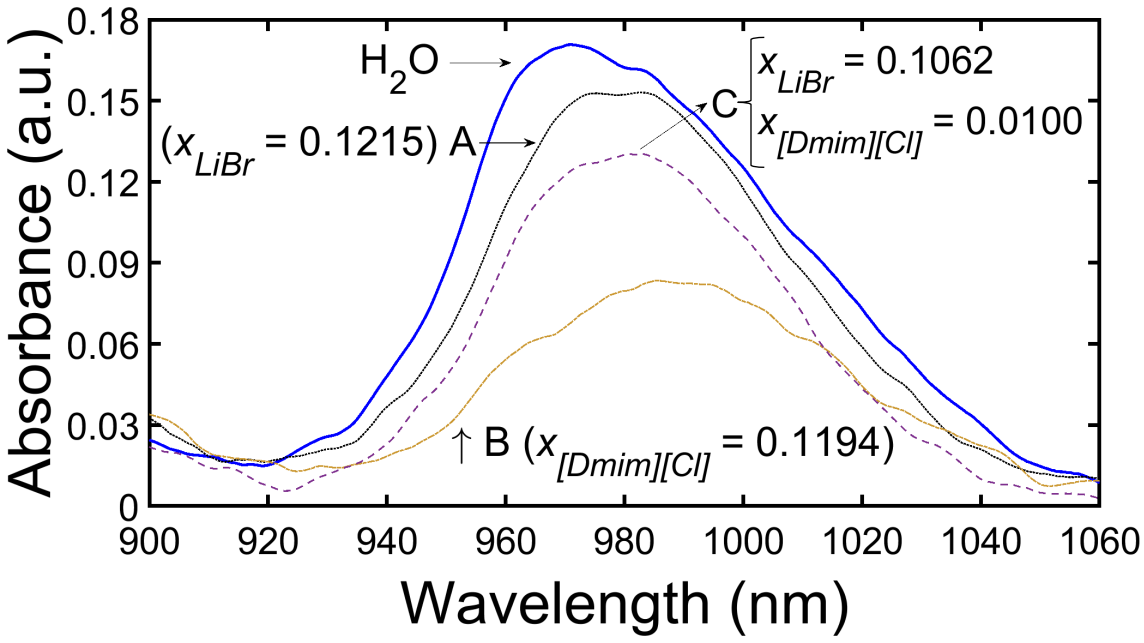

Figure 2. Experimental spectra of water and mixtures with relatively similar absorbent concentration. (A (…) (H_2O+LiBr; x_{LiBr} = 0.1215); B(–) (H_2O+[Dmim][Cl]; $x_{[Dmim][Cl]}$ = 0.1162); C(---) (H_2O+LiBr+[Dmim][Cl]; x_{LiBr} = 0.1062 + $x_{[Dmim][Cl]}$ = 0.0100)).

The comparison between spectra A and B with respect to the water spectrum reveals that the effect of the absorbent concentration in the intensity decrease and displacement of the water absorption band is significantly more important for [Dmim][Cl] solutions than for LiBr ones. Therefore, the water affinity of this IL is higher than that of lithium bromide.

Focusing the attention on the composition of the mixtures of the C spectrum (x_{LiBr} = 0.1062; $x_{[Dmim][Cl]}$ = 0.0100) and A spectrum (x_{LiBr} = 0.1215), it is observed that although the lithium bromide mole fraction is 0.0153 lower in the former, this difference is almost compensated by the presence of the IL, which is a better absorbent. According to that, the intensity decrease in the water absorption band in the ternary mixture (C) cannot be explained solely by its lower absorbent mole fraction. This behavior could be a consequence of the interaction between both the lithium bromide and the IL.

A more accurate analysis is obtained by comparing the amount of water that remains as bulk water in the mixtures as a function of the absorbent concentration. According to what was shown in previous works [17,18], this information is obtained from multivariate curve resolution of the individual spectra data matrices: $\mathbf{M}_{H2O+LiBr+[Dmim][Cl]}$, $\mathbf{M}_{H2O+LiBr}$ and $\mathbf{M}_{H2O+[Dmim][Cl]}$. During the resolution and according to

indicated in section 2.3, the number of factors required to keep almost the total variability of the spectra data has been determined from the results of the singular value decomposition (SVD) of the data matrices. That occurs with two factors in the individual data matrices $\mathbf{M}_{H2O+LiBr}$ and $\mathbf{M}_{H2O+[Dmim][Cl]}$ (99.98 % and 99.97 % variance represented, respectively), and with three factors in the data spectra matrix $\mathbf{M}_{H2O+LiBr+[Dmim][Cl]}$ (99.94 % variance represented). In all cases, the concentration profiles obtained by evolving factors analysis (EFA) of the data matrices with the indicated factors were used to initialize the MCR-ALS algorithm. The lack of fit of the final solutions was always lower than 2.53 %.

Figure 3 shows the solutions of spectral (a, c, e) and concentration (b, d, f) profiles recovered by MCR-ALS for $\mathbf{M}_{H2O+LiBr,}$ (a, b), $\mathbf{M}_{H2O+[Dmim][Cl}$ (c, d) and $\mathbf{M}_{H2O+LiBr+[Dmim][Cl]}$ (e, f).

Figure 3. Spectral (a, c, e) and concentration (b, d, f) profiles recovered by MCR-ALS for $M_{H2O+LiBr,}$ (a, b), $M_{H2O+[Dmim][Cl]}$ (c, d) and $M_{H2O+LiBr+[Dmim][Cl]}$ (e, f).

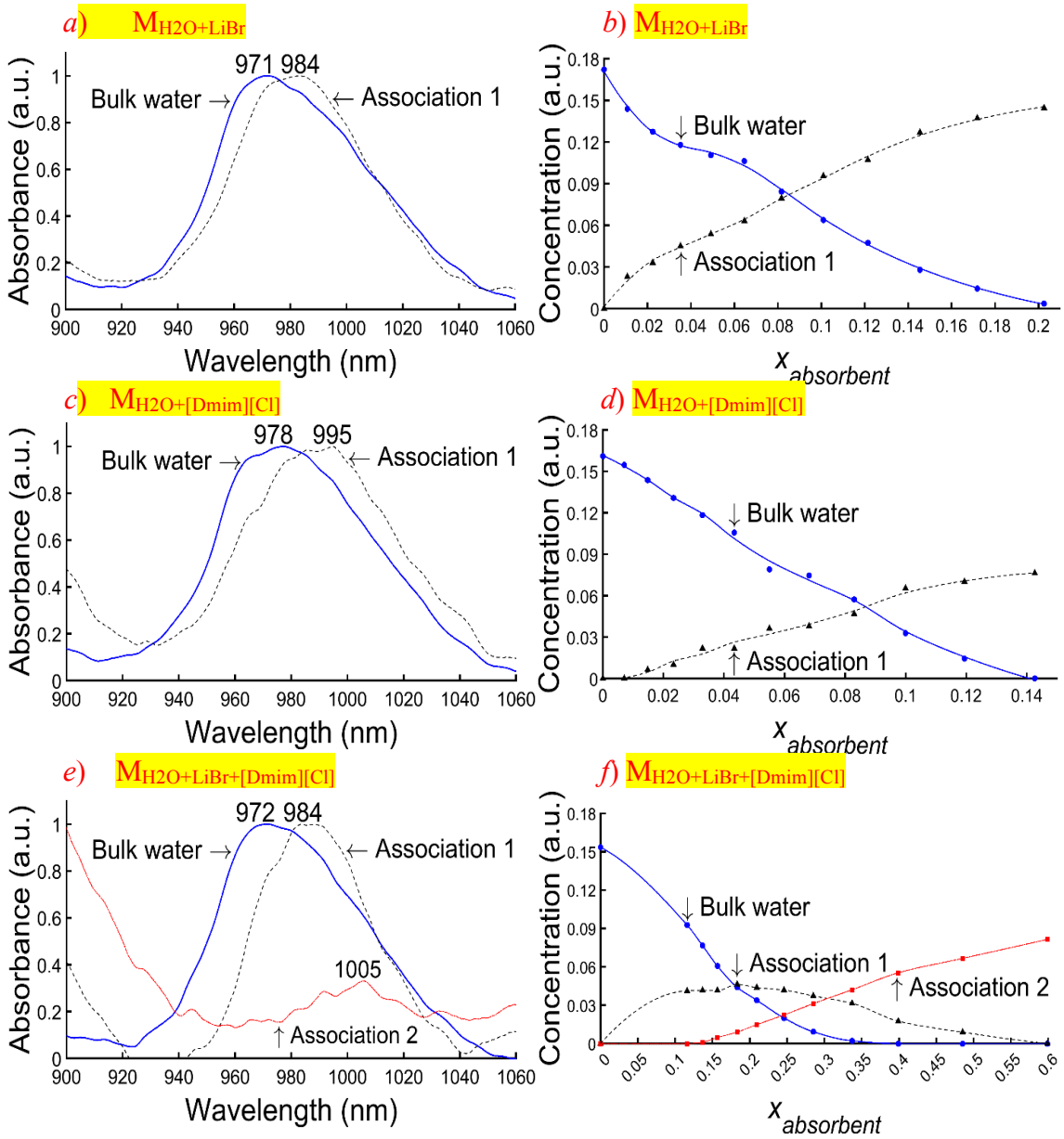

The similarity coefficient between the recovered spectrum with the maximum around 973 nm in the spectral plots (a, c, e) and the pure water spectrum is always higher than 0.999, so it can be considered representative of bulk water in the solutions. The other recovered spectra, labeled as "Association 1" and "Association 2" in the different plots, exhibit the peak displacement towards longer wavelengths, and they can be considered representative of water molecules involved in the hydration of the ions [17,18]. It is not possible to determine the different structural conformations representative of the ions in the solvated structure solely from NIR spectra information.

The concentration profiles recovered by MCR-ALS for bulk water and Associations are represented in plots (b, d and f), as a function of the absorbent mole fraction in the solutions (LiBr or [Dmim][Cl] in plots b) and d), respectively, or LiBr+[Dmim][Cl] in plot f)). A detailed inspection of the plots reveals the presence of different water chemical environments in the solutions as a function of the absorbent mole concentration. For example, in plot f) it is possible to observe that in (H_2O+LiBr+[Dmim][Cl]) solutions, when the IL mole fraction is lower than 0.0100 ($x_{absorbent} < 0.1161$) it can be assumed that bulk water molecules coexist with water molecules solvating the ions of LiBr, Association 1. When the IL concentration increases ($0.1161 < x_{absorbent} < 0.3992$), the molecules of bulk water coexist also with water molecules solvating the ions of LiBr and [Dmim][Cl], labelled as Association 1 and Association 2. At higher IL mole fraction in the solutions ($x_{absorbent} > 0.3992$) there is no bulk water. Similar considerations that were done and discussed in previous works [17,18] can be done for the binary mixtures too.

The most interesting aspect is that we can now visualize the evolution of the bulk water concentration in these mixtures and use the percentage that remains as bulk water in each solution to compare the amount of water involved in the solvation of the ions in ternary solutions compared to the binary solutions. According to Beer law, the MCR-ALS recovered values are proportional to the mole concentration values of bulk water and water associated, so they are also proportional to their mole fraction values in the mixtures. With this consideration, the percentage of bulk water in the mixtures was calculated as (% bulk water = $100 \cdot (x_{H2O\ recovered}/x_{H2O})$. Firstly, in the calculation, the concentration values of bulk water shown in plots (b, d, and f) of Figure 3 were normalized using the value of the pure water as reference (the first mixture included in the corresponding spectral data matrix). The coefficient of the normalized concentration values ranged between 1 and 0. Secondly, in each solution the $x_{H2O\ recovered}$ value is

calculated by multiplying each coefficient by x_{H2O} in the prepared solutions. The water mole fraction that participates in the associations, named $x_{H2O\ associated}$, is determined as the difference between $x_{H2O} - x_{H2O\ recovered}$. Table 3 reports these values for binary and ternary mixtures.

Table 3. Absorbent and water mole fraction values in the prepared mixtures and bulk and associated water mole fraction calculated from MCR-ALS results for a) (H_2O+LiBr) mixtures b) (H_2O+[Dmim][Cl]) and c) (H_2O+LiBr+[Dmim][Cl]).

a) (H_2O+LiBr)				*b*) (H_2O+[Dmim][Cl])				*c*) (H_2O+LiBr+[Dmim][Cl])			
Prepared mixtures		Values from MCR-ALS		Prepared mixtures		Values from MCR-ALS		Prepared mixtures		Values from MCR-ALS	
$x_{absorbent} = x_{LiBr}$	x_{H2O}	x_{H2O} *recovered*	x_{H2O} associated	$x_{absorbent} = x_{[Dmim][Cl]}$	x_{H2O}	x_{H2O} *recovered*	x_{H2O} associated	$x_{absorbent} = x_{LiBr}+x_{[Dmim][Cl]}$	x_{H2O}	x_{H2O} *recovered*	x_{H2O} associated
0	1	1	0	0	1	1	0	0	1	1	0
0.0108	0.9892	0.8265	0.1627	0.0071	0.9929	0.9538	0.0391	0.1162	0.8838	0.5338	0.3500
0.0224	0.9776	0.7237	0.2539	0.0149	0.9851	0.8785	0.1066	0.1368	0.8632	0.4306	0.4326
0.0352	0.9648	0.6615	0.3033	0.0233	0.9767	0.7931	0.1836	0.1568	0.8432	0.3332	0.5100
0.0492	0.9508	0.6105	0.3403	0.0329	0.9671	0.7103	0.2568	0.1832	0.8168	0.2341	0.5827
0.0646	0.9354	0.5780	0.3574	0.0434	0.9566	0.6269	0.3297	0.2094	0.7906	0.1748	0.6158
0.0817	0.9183	0.4504	0.4679	0.0550	0.9450	0.4643	0.4807	0.2458	0.7542	0.0984	0.6558
0.1011	0.8989	0.3341	0.5648	0.0681	0.9319	0.4322	0.4997	0.2851	0.7149	0.0430	0.6719
0.1215	0.8785	0.2425	0.6360	0.0830	0.9170	0.3258	0.5912	0.3373	0.6627	0.0092	0.6535
0.1455	0.8545	0.1394	0.7151	0.1000	0.9000	0.1835	0.7165	0.3992	0.6008	0	0.6008
0.1718	0.8282	0.0697	0.7585	0.1194	0.8806	0.0785	0.8021	0.4852	0.5148	0	0.5148
0.2026	0.7974	0.0171	0.7803	0.1426	0.8574	0	0.8574	0.5987	0.4013	0	0.4013

To discuss the results, in Figure 4 we have represented the percentage of bulk water as a function of the absorbent mole fraction in the different mixtures. In order to facilitate the discussion, the mixtures A, B, and C – previously discussed in Figure 3 – are included along with points D and E, which are representative of cases that will be discussed later.

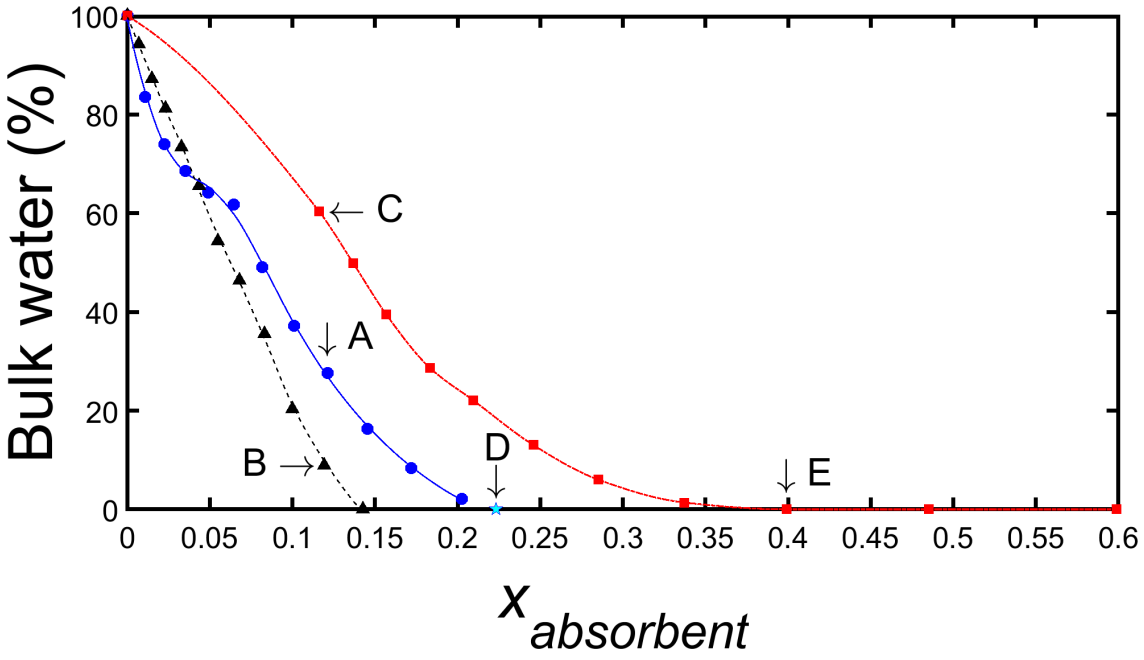

Figure 4. Percentage of bulk water as a function of the absorbent mole fraction in: (● : H_2O+LiBr) mixtures, (▲ : H_2O+[Dmim][Cl]) and (■: H_2O+LiBr+[Dmim][Cl]) mixtures.

Before focusing on ternary mixtures, we have compared the results of binary mixtures with those reported in the literature. For example, for the lithium bromide mixtures, it can be expected that the mole fraction x_{LiBr} at which the percentage of bulk water is zero agrees with the saturated conditions of (H_2O+LiBr) at 25 ºC. We can estimate this value – point (D) – by extrapolating the experimental values of the lithium bromide data series. The obtained lithium bromide mole fraction is $x_{LiBr} = 0.2264$, which is representative of mixtures with a 1 LiBr : 3.4 H_2O mole ratio, and is in good agreement with the information in the literature at similar temperature ($T = 24.29$ ºC, $x_{LiBr} = 0.2421$, 1 LiBr : 3.1 H_2O) [43].

The strong slope of the bulk water values in the IL series confirms its high affinity to water, which is attributable to the short length of the alkyl chain [44]. It can be observed

that the zero value is achieved for a mixture with relatively low concentration ($x_{[Dmim][Cl]}$ = 0.1426).

Focusing the attention on the evolution of bulk water in the (H_2O+LiBr+[Dmim][Cl]) mixtures, the following aspects can be easily visualized:

a) At similar absorbent mole fraction, the amount of water that remains in the mixtures as bulk water decreases in the following order: (H_2O+LiBr+[Dmim][Cl]) > (H_2O+LiBr) > (H_2O+ Dmim][Cl]). As an example, now it is possible to highlight the small differences between the absorbent concentration of the binary mixture A (x_{LiBr} = 0.1215) and the ternary mixture C (x_{LiBr} + $x_{[Dmim][Cl]}$ = 0.1062 + 0.0100), given the surprisingly high difference (32.8 %) of their percentages of bulk water, (27.6 % vs 60.4 %), considering the presence of the IL. The percentage of bulk water of the ternary mixture C (60.4 %) is the one that would have a (H_2O+LiBr) mixture with x_{LiBr} < 0.065, which is a significant lower lithium bromide mole fraction than in mixture C.

b) The zero value of bulk water percentage is achieved in the mixture with absorbent mole fraction $x_{absorbent}$ = 0.3992, point E in Fig 4, in which the lithium bromide mole fraction is x_{LiBr} = 0.2162. This lithium bromide mole fraction is far from the compositions of the two last ternary mixtures prepared (x_{LiBr} = 0.2516 and x_{LiBr} = 0.2944), in which x_{LiBr} overcomes the estimated value at saturated solution conditions in the binary mixtures, shown at point D.

A possible explanation to that is the formation of ionic aggregates because of the interactions between the ions of LiBr and [Dmim][Cl]. These interactions facilitate to dissolve a greater amount of LiBr in the solution when the IL is added, similarly to what was referenced for the lithium nitrate in the presence of protic ILs [45].

A deeper insight into the molecular interaction between H_2O–LiBr–[Dmim][Cl] in these mixtures has been done in the next section using computational studies. However, before concluding the exposition of the NIR-MCR-ALS results, we present information regarding the number of water molecules per mole of absorbent in the solvated structures (n) formed in binary and ternary mixtures in Figure 5, in which we have represented the quotient n – calculated as $x_{H2O\ associated}/x_{absorbent}$ using the data of Table 3 – against the mole fraction of absorbent.

It can be observed that in the (H_2O+LiBr) prepared mixtures, the mole ratio n varies significantly with the x_{LiBr}, from n = 15.1 in the most diluted mixture (x_{LiBr} = 0.0108) to n = 3.9 in the most concentrated solution (x_{LiBr} = 0.2026). This value agrees

with the expected considering that the x_{LiBr} of this mixture is slightly higher than that of the saturated solution (x_{LiBr} = 0.2421), that is 1 LiBr : 3.1 H_2O [43].

In the (H_2O+[Dmim][Cl]) mixtures, the mole ratio ranges between 8.0 and 6.0 over the entire concentration range. This variation is not as pronounced as that of lithium bromide solutions, which is indicative of a significantly different solvation process of the ions with respect to the inorganic salts.

In the (H_2O+LiBr+[Dmim][Cl]) mixtures, the mole ratio is always significantly lower than in lithium bromide solutions. As an example, for the ternary mixture with $x_{absorbent}$ = 0.1568 (x_{LiBr} = 0.1229 + $x_{[Dmim][Cl]}$ = 0.0339), the calculated n is 3.3, while for the (H_2O+LiBr) mixture with x_{LiBr} = 0.1718 the calculated mole ratio is 4.4. A low n value of 0.7 is observed in the most concentrated ternary mixture with $x_{absorbent}$ = 0.5987 (x_{LiBr} = 0.2944 + $x_{[Dmim][Cl]}$ = 0.3043). This behavior is consistent with the abovementioned formation of aggregates [45] where LiBr is interacting not only with H_2O, but also with [Dmim][Cl].

These results, which are not straightforward to interpret with the NIR-MCR-ALS data alone, could be better understood when combined with the computational analysis discussed below.

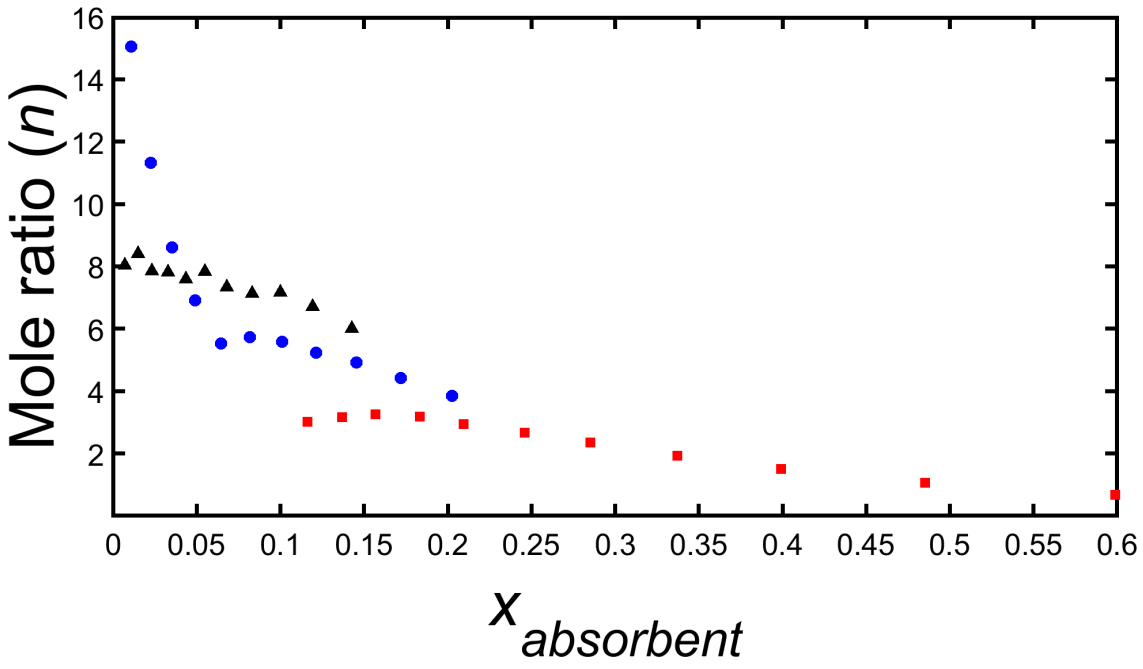

Figure 5. Mole ratio (H_2O/absorbent) in the formed solvated structures as a function of absorbent mole fraction for: (●: H_2O+LiBr), (▲:H_2O+[Dmim][Cl]) and (■: H_2O+LiBr+[Dmim][Cl]) mixtures.

3.2 Structural analysis of LiBr-[Dmim][Cl]-H_2O mixtures from MD simulations.

To computationally characterise the microscopical structure of the mixtures, we calculated the radial distribution functions (RDFs, *g(r)*) between the different types of molecules for all the simulated concentrations. The RDF of molecules B in a shell at distance *r* around a molecule A are obtained from the production runs as:

$$g_{AB}(r) = \frac{V}{N_A N_B} \sum_{i=1}^{N_A} \sum_{j=1}^{N_B} \langle \delta(|\boldsymbol{r}_i - \boldsymbol{r}_j| - r) \rangle$$

For the RDFs involving H_2O molecules, the oxygen atom was considered for the calculations. From the RDFs, we also computed the running coordination number (*n(r)*), that is, the average number of molecules B around a central molecule A within a distance *r*:

$$n(r) = \frac{N_B}{V} \int_0^r 4\pi (r')^2 g_{AB}(r') dr'$$

The coordination number (CN), i.e., the number of molecules B in the first solvation shell of a molecule A, is $n(r_1)$, r_1 being the position of the first minimum in the corresponding $g(r)$.

In Figure 6 we can observe the concentration dependence of the RDFs between water molecules around some of the species present in the ternary mixtures (Br (a), Cl (b), H_2O (c) and Li (d)). In addition, the corresponding running coordination numbers are included in the insets. It can be seen that there is a strong interaction between water and lithium cations. With regard to the RDF-Li-H_2O, a local minimum clearly exists between the first peaks (r ~ 1.9 Å) and the second peaks (r ~ 4.0 Å). In addition, the shape of this g(r) does not change significantly with the concentration of the ternary mixture, which shows that the solvation structure around lithium is not influenced by its surroundings. We can also observe that both Br and Cl show to possess an environment in which water molecules are located at greater distances (r ~ 3.3 Å and r ~ 3.1 Å, respectively) than in the case of lithium. Moreover, in these cases the local minimum beyond the first peak is more pronounced as the mixture becomes more concentrated, which means that the hydration water molecules can be more clearly distinguished from the surrounding ones than in the diluted solutions. These observations are in good agreement with previous studies reporting the hydration structure of inorganic salts in water [46,47]. As the experimental measurements previously described, our simulations also show different water environments in the solutions as a function of the absorbent mole concentration, with a remarkable preference to be coordinated with lithium cations but remaining partially coordinated to other water molecules through an extended hydrogen-bond network. In fact, the first solvation shell of water evolves from having 4 water molecules in pure water (Figure S1), to continuing to be mainly free of the monoatomic ions but incorporating some of them to its tetrahedral structure at different distances (the closest one being Li) with $x_{absorbent} = 0.1161$ and to being surrounded by only 1 H_2O and several ions when the concentration increases up to $x_{absorbent} = 0.5987$, when the original structural properties of pure water have already disappeared. This behaviour can be considered representative of bulk water decreasing with increasing the absorbent mole fraction.

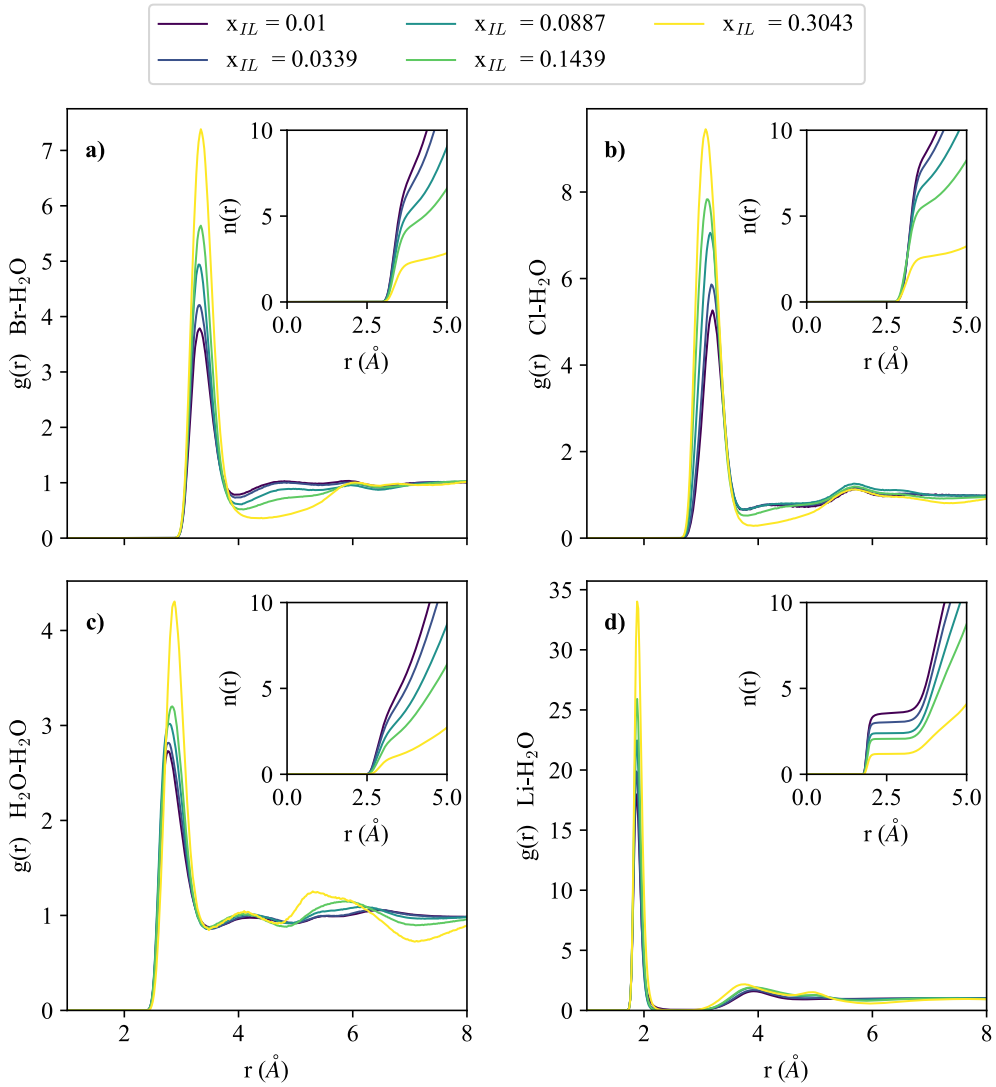

Figure 6. RDFs between water molecules and Br (a), Cl (b), H_2O (c) and Li (d) as a function of the IL mole fraction in the ternary mixtures. The insets show the evolution of the running coordination numbers of water molecules around the other species identified in the RDFs.

Since water exhibits a preferential coordination with lithium cations in the ternary mixtures, we analysed the possible formation of ionic aggregates of this ion through the concentration dependence of its first solvation layer. These results are included in Figure 7, and it can be seen that in the most diluted system the first solvation shell of lithium is made of, on average, almost 4 water molecules and 0.5 bromides, water being located at closer distances. For the highest simulated concentration of absorbent, lithium shows to be surrounded by approximately 1 H_2O, 2 Cl and 1 Br. In this case, the ratio of ions and water molecules is 1:1.3 and the hydration numbers of the ions are between 1 and 2, which means that most water molecules are hydration water and not bulk water in line with

experiments. From Figure 7 we can also conclude that higher interaction between the ions appears with increasing the absorbent mole fraction, which is in agreement again with the experimental findings.

To complement classical MD results, we have also performed Car-Parrinello MD simulations, which are within the group of so-called first-principles or *ab initio* MD (AIMD) and allow for a non-biased full-quantum description of the electrons in the system in contrast to classical MD that rely on pre-built force fields. Therefore, in this way the electronic structure and the molecular interactions are described at DFT level (PBE functional, see 2.4 Computational details). The size of the simulated system and the simulation time, compared to classical MD, are much smaller tough, so the two types of MD simulations (first-principles and classical) are in some way complementary. We have simulated two different concentrations of absorbent, a diluted solution ($x_{[Dmim][Cl]}$ = 0.0357, $x_{absorbent}$ = 0.1429) and a concentrated solution ($x_{[Dmim][Cl]}$ = 0.3000, $x_{absorbent}$ = 0.6000). The results confirm the coordination number of 4 for Li ions, as found by MD with only slight differences in the Li-Br, Li-Cl and Li-H_2O RDFs and coordination numbers (see Figure S3). For the diluted solution, four water molecules are coordinated to Li in the first shell with no coordination of chloride nor bromide anions, as clearly shown in Figure 8a where a snapshot of the simulation is represented. For the concentrated solution, the coordination numbers are approximately *n(Li-Cl) = 2*, *n(Li-Br) = 1.5* and *n(Li-H_2O) = 0.5*, very similar to those found in MD with bromide anions somewhat more favored than water. Figure 8b shows one representative snapshot of the CPMD trajectory for the concentrated solution.

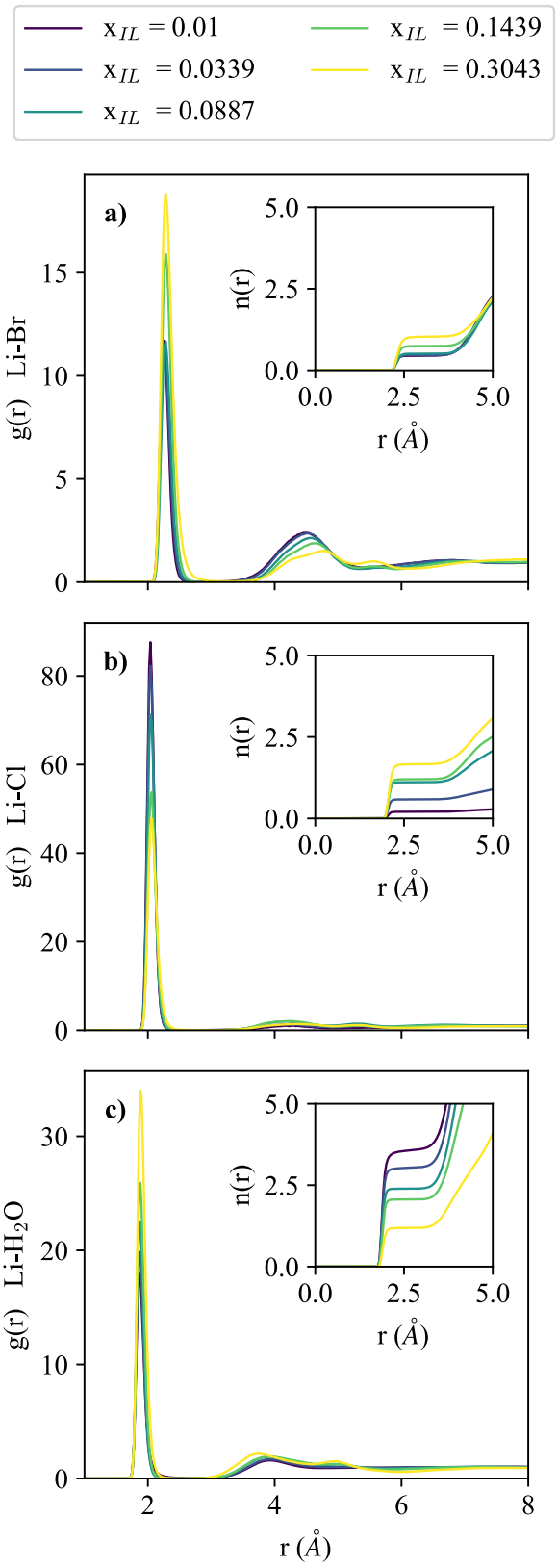

Figure 7. RDFs between Li cations and Br (a), Cl (b) and H_2O (c) as a function of the IL mole fraction in the ternary mixtures. The insets show the evolution of the running coordination numbers of the species identified in the RDFs around a central lithium atom.

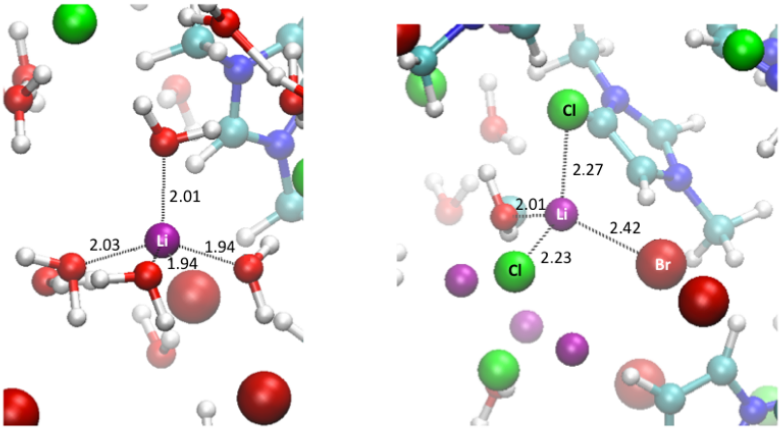

(a) (b)

Figure 8. Structure of the first solvation shell of Li ion in a snapshot of the CPMD trajectory (a) diluted solution and (b) concentrated solution. Color code for the atoms: Li (magenta), Br (dark red), Cl (green), O (red), C (light blue), N (dark blue), H (white). Distances are in Angstrom.

We also examined the concentration dependence of single-particle dynamics of some species of the ternary mixtures by means of classical MD, which can provide us with useful information about the correlations of the molecules in their solvation cages. For that purpose, we computed the Fourier transform of the normalized velocity autocorrelation functions, which is the vibrational Density of States (vDos):

$$I(\omega) = \int_0^\infty e^{-i\omega t} \frac{\langle \boldsymbol{v}(t) \cdot \boldsymbol{v}(0) \rangle}{\langle \boldsymbol{v}(0) \cdot \boldsymbol{v}(0) \rangle} dt$$

It must be noted that in the case of water molecules these properties were evaluated using their centre of mass. Moreover, we follow the convention here that *I(ω)* is normalized such that

$$\int_0^\infty I(\omega) d\omega = 1$$

The concentration dependence of the vDos of Br (a), Cl (b), H_2O (c) and Li (d) are plotted in Figure 9. Focusing on water molecules, we can observe that the vibrational mode at low frequencies that is characteristic of pure water (Figure S2) and is still visible in the more diluted solutions, decreases with increasing the absorbent mole fraction. In fact, for the system with $x_{absorbent}$ = 0.5987 this mode has completely disappeared, and water molecules only show a vibrational mode at higher frequencies that has increased with concentration. This is consistent with those hydration waters in the concentrated solution being surrounded by lithium cations at closer distances, which induces a rattling

motion of H_2O due to a pronounced caging effect. The opposite behaviour can be inferred for lithium cations, which exhibit a new vibrational mode at low frequencies when $x_{absorbent} = 0.5987$. This is due to a "loosening" of its first solvation shell as it goes from being occupied by 4 close waters at "infinite" dilution to ions at longer distances in concentrated solutions.

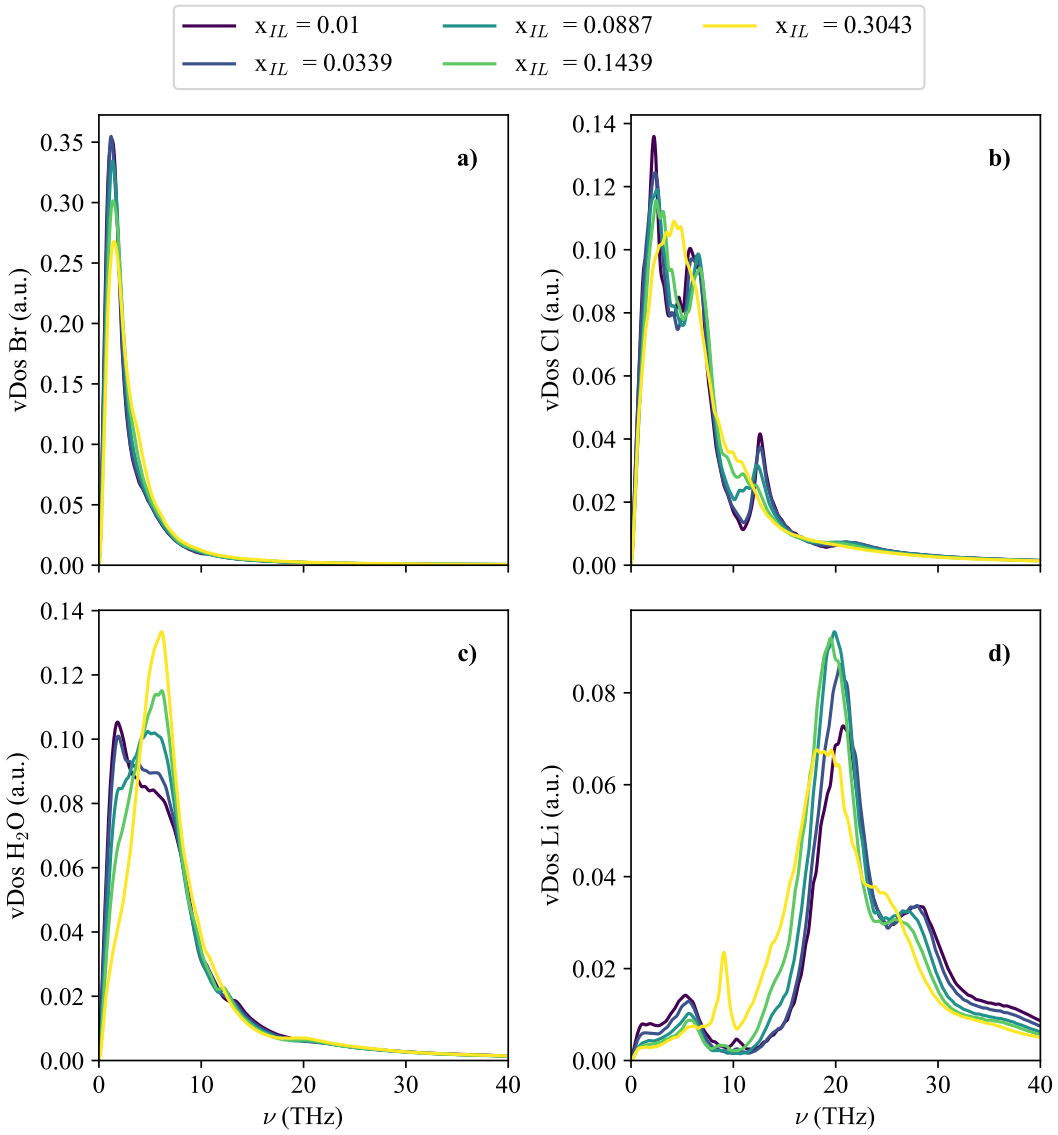

Figure 9. vDos of some of the species that are present in the ternary mixtures as a function of the IL mole fraction. The spectrum was smoothed using a low-pass filter with a cut-off frequency of 1.5 THz.

4. Conclusions

In this work, the water association in ternary (H_2O+LiBr+[Dmim][Cl]) mixtures have been quantitatively and structurally analyzed using curve resolution (MCR-ALS) of NIR spectra and molecular dynamics (MD) simulations, including Classical and Car-Parrinello approaches. NIR spectra of the ternary mixtures prepared with absorbent mole fraction (LiBr+[Dmim][Cl]) from 0 to 0.5987 (x_{LiBr} = 0.2944 + $x_{[Dmim][Cl]}$ = 0.3043) and the MD simulations were carried out at selected compositions within this concentration range.

The results revealed the existence of three water chemical environments in our ternary mixtures: bulk water in absence of solutes, bulk water coexisting with solvated water and solvated water.

The comparative analysis of these results with those obtained for binary mixtures (H_2O+LiBr) and (H_2O+[Dmim][Cl]) evidenced that the water amount that remains as bulk water in ternary solutions is higher than in binary mixtures. In the comparative analysis, at similar absorbent mole fraction, the bulk water decreases in the following order: (H_2O+LiBr+[Dmim][Cl]) > (H_2O+LiBr) > (H_2O+[Dmim][Cl]).

The existence of chemical environments without bulk water and with a higher lithium mole fraction than the referenced at saturated conditions for the (H_2O+LiBr) is attributed to the presence of ionic aggregates, which facilitates to dissolve a higher concentration of lithium bromide as a result of the interactions between LiBr and [Dmim][Cl].

In the considered concentration range, the mole ratio between the H_2O/absorbent in ternary mixtures is significantly lower than in binary mixtures, evidencing again the existence of interactions between lithium bromide and the ionic liquid.

MD simulations (including both classical and Car-Parrinello approaches) were also performed to explore the detailed structure of the ternary mixtures, and they showed to be in line with the experimental results. Classical MD simulations for five different concentrations with mole fraction of absorbent (x_{LiBr}+$x_{[Dmim][Cl]}$) ranging between 0.1161 and 0.5987 confirmed that water environment evolves from being essentially coordinated with other water molecules in the most diluted system, to being mainly surrounded by monoatomic ions (lithium showing a preferential interaction at close distances) for the

most concentrated mixture. At that point, we can state that there are almost no bulk water molecules and most of them can be considered as hydration waters. Furthermore, higher interaction between the ions appears with increasing the absorbent mole fraction, which is confirmed by CPMD simulations and in line with the higher amount of bulk water in ternary than in binary solutions.

References

[1] L. Jing, Z. Danxing, F. Lihua, W. Xianghong, D. Li, Vapor pressure measurement of the ternary systems H2O + LiBr + [Dmim]Cl, H2O + LiBr + [Dmim]BF4, H2O + LiCl + [Dmim]Cl, and H2O + LiCl + [Dmim]BF4, J Chem Eng Data. 56 (2011) 97–101. https://doi.org/10.1021/je1009202.

[2] K.-S. Kim, D. Demberelnyamba, B.-K. Shin, S.-H. Yeon, S. Choi, J.-H. Cha, H. Lee, C.-S. Lee, J.-J. Shim, Surface tension and viscosity of 1-butyl-3-methylimidazolium iodide and 1-buyl-3-methylimidazolium tetrafluoborate, and solubility of lithium bromide+1-butyl-3-methylimidazolium bromide in water, Korean Journal of Chemical Engineering. 23 (2006) 113–116.

[3] M.T. Zafarani-Moattar, F. Frouzesh, The study of vapor-liquid equilibria of 1-ethyl-3-methyl imidazolium chloride and 1-butyl-3-methyl imidazolium chloride in lithium bromide aqueous solutions and their corresponding binary systems at 298.15 K., CALPHAD. 40 (2013) 16–23. https://doi.org/10.1016/j.calphad.2012.11.002.

[4] M. Królikowska, T. Hofman, The influence of bromide-based ionic liquids on solubility of {LiBr (1) + water (2)} system. Experimental (solid + liquid) phase equilibrium data. Part 1, J Mol Liq. 273 (2019) 606–614. https://doi.org/10.1016/j.molliq.2018.09.104.

[5] M. Królikowska, M. Zawadzki, M. Skonieczny, The influence of bromide-based ionic liquids on solubility of {LiBr (1) + water (2)} system. Experimental (solid + liquid) phase equilibrium data. Part 2, J Mol Liq. 265 (2018) 316–326. https://doi.org/10.1016/j.molliq.2018.06.006.

[6] A.B. Pereiro, J.M.M. Araújo, F.S. Oliveira, J.M.S.S. Esperança, J.N. Canongia Lopes, I.M. Marrucho, L.P.N. Rebelo, Solubility of inorganic salts in pure ionic

liquids, Journal of Chemical Thermodynamics. 55 (2012) 29–36. https://doi.org/10.1016/j.jct.2012.06.007.

[7] T. Köddermann, C. Wertz, A. Heintz, R. Ludwig, The association of water in ionic liquids: A reliable measure of polarity, Angewandte Chemie - International Edition. 45 (2006) 3697–3702. https://doi.org/10.1002/anie.200504471.

[8] T. Singh, A. Kumar, Aggregation behavior of ionic liquids in aqueous solutions: Effect of alkyl chain length, cations, and anions, Journal of Physical Chemistry B. 111 (2007) 7843–7851. https://doi.org/10.1021/jp0726889.

[9] L. Cammarata, S.G. Kazarian, P.A. Salter, T. Welton, Molecular states of water in room temperature ionic liquids, Physical Chemistry Chemical Physics. 3 (2001) 5192–5200. https://doi.org/10.1039/b106900d.

[10] T.L. Greaves, D.F. Kennedy, A. Weerawardena, N.M.K. Tse, N. Kirby, C.J. Drummond, Nanostructured protic ionic liquids retain nanoscale features in aqueous solution while precursor Brønsted acids and bases exhibit different behavior, Journal of Physical Chemistry B. 115 (2011) 2055–2066. https://doi.org/10.1021/jp1112203.

[11] R. Hayes, S. Imberti, G.G. Warr, R. Atkin, How water dissolves in protic ionic liquids, Angewandte Chemie - International Edition. 51 (2012) 7468–7471. https://doi.org/10.1002/anie.201201973.

[12] B. Docampo-Álvarez, V. Gómez-González, T. Méndez-Morales, J. Carrete, J.R. Rodríguez, Ó. Cabeza, L.J. Gallego, L.M. Varela, Mixtures of protic ionic liquids and molecular cosolvents: A molecular dynamics simulation, Journal of Chemical Physics. 140 (2014). https://doi.org/10.1063/1.4879660.

[13] A.K. Soper, Partial structure factors from disordered materials diffraction data: An approach using empirical potential structure refinement, Phys Rev B Condens Matter Mater Phys. 72 (2005). https://doi.org/10.1103/PhysRevB.72.104204.

[14] J. Jaumot, A. de Juan, R. Tauler, MCR-ALS GUI 2.0: New features and applications, Chemometrics and Intelligent Laboratory Systems. 140 (2015) 1–12. https://doi.org/10.1016/j.chemolab.2014.10.003.

[15] M. López-Pastor, M.J. Ayora-Cañada, M. Valcárcel, B. Lendl, Association of methanol and water in ionic liquids elucidated by infrared spectroscopy using two-dimensional correlation and multivariate curve resolution, Journal of Physical Chemistry B. 110 (2006) 10896–10902. https://doi.org/10.1021/jp057398b.

[16] A.A. Gowen, J.M. Amigo, R. Tsenkova, Characterisation of hydrogen bond perturbations in aqueous systems using aquaphotomics and multivariate curve resolution-alternating least squares, Anal Chim Acta. 759 (2013) 8–20. https://doi.org/10.1016/j.aca.2012.10.007.

[17] M.I. Barba, M.S. Larrechi, A. Coronas, Quantitative analysis of the hydration of lithium salts in water using multivariate curve resolution of near-infrared spectra, Anal Chim Acta. 919 (2016) 20–27. https://doi.org/10.1016/j.aca.2016.03.022.

[18] M.I. Barba, M.S. Larrechi, A. Coronas, Quantitative analysis of free water in ionic liquid-water mixtures, Talanta. 199 (2019) 407–414. https://doi.org/10.1016/j.talanta.2019.02.087.

[19] J.M. Otero-Mato, V. Lesch, H. Montes-Campos, J. Smiatek, D. Diddens, O. Cabeza, L.J. Gallego, L.M. Varela, Solvation in ionic liquid-water mixtures: A computational study, J Mol Liq. 292 (2019). https://doi.org/10.1016/j.molliq.2019.111273.

[20] T. Méndez-Morales, J. Carrete, S. Bouzón-Capelo, M. Pérez-Rodríguez, Ó. Cabeza, L.J. Gallego, L.M. Varela, MD simulations of the formation of stable clusters in mixtures of alkaline salts and imidazolium-based ionic liquids, Journal of Physical Chemistry B. 117 (2013) 3207–3220. https://doi.org/10.1021/jp312669r.

[21] P. Martínez-Crespo, M. Otero-Lema, O. Cabeza, H. Montes-Campos, L.M. Varela, Structure, dynamics and ionic conductivities of ternary ionic liquid/lithium salt/DMSO mixtures, J Mol Liq. 359 (2022). https://doi.org/10.1016/j.molliq.2022.119188.

[22] B. Slutsky, Handbook of Chemometrics and Qualimetrics: Part A By D. L. Massart, B. G. M. Vandeginste, L. M. C. Buydens, S. De Jong, P. J. Lewi, and J. Smeyers-Verbeke. Data Handling in Science and Technology Volume 20A.

Elsevier: Amsterdam. 1997. Xvii + 867 pp. ISBN 0-444-89724-0. $293.25., J Chem Inf Comput Sci. 38 (1998) 1254–1254. https://doi.org/10.1021/ci980427d.

[23] M. Maeder, A.D. Zuberbuehler, The resolution of overlapping chromatographic peaks by evolving factor analysis, Anal Chim Acta. 181 (1986) 287–291.

[24] D. van der Spoel, E. Lindahl, B. Hess, G. Groenhof, A.E. Mark, H.J.C. Berendsen, GROMACS: Fast, flexible, and free, J Comput Chem. 26 (2005) 1701–1718. https://doi.org/10.1002/jcc.20291.

[25] M.J. Abraham, T. Murtola, R. Schulz, S. Páll, J.C. Smith, B. Hess, E. Lindah, Gromacs: High performance molecular simulations through multi-level parallelism from laptops to supercomputers, SoftwareX. 1–2 (2015) 19–25. https://doi.org/10.1016/j.softx.2015.06.001.

[26] W.L. Jorgensen, D.S. Maxwell, J. Tirado-Rives, Development and Testing of the OPLS All-Atom Force Field on Conformational Energetics and Properties of Organic Liquids, J Am Chem Soc. 118 (1996) 11225–11236. https://pubs.acs.org/sharingguidelines.

[27] B. Doherty, X. Zhong, S. Gathiaka, B. Li, O. Acevedo, Revisiting OPLS Force Field Parameters for Ionic Liquid Simulations, J Chem Theory Comput. 13 (2017) 6131–6135. https://doi.org/10.1021/acs.jctc.7b00520.

[28] J.N. Canongia Lopes, J. Deschamps, A.A.H. Pádua, Modeling Ionic Liquids Using a Systematic All-Atom Force Field, Journal of Physical Chemistry B. 108 (2004) 2038–2047. https://doi.org/10.1021/jp0362133.

[29] M.W. Mahoney, W.L. Jorgensen, A five-site model for liquid water and the reproduction of the density anomaly by rigid, nonpolarizable potential functions, Journal of Chemical Physics. 112 (2000) 8910–8922. https://doi.org/10.1063/1.481505.

[30] L. Martinez, R. Andrade, E.G. Birgin, J.M. Martínez, PACKMOL: A package for building initial configurations for molecular dynamics simulations, J Comput Chem. 30 (2009) 2157–2164. https://doi.org/10.1002/jcc.21224.

[31] E.. J. Haug, J.S. Arora, K. Matsui, A Steepest-Descent Method for Optimization of Mechanical Systems, J Optim Theory Appl. 19 (1976) 401–424.

[32] G. Bussi, D. Donadio, M. Parrinello, Canonical sampling through velocity rescaling, Journal of Chemical Physics. 126 (2007). https://doi.org/10.1063/1.2408420.

[33] M. Parrinello, A. Rahman, Polymorphic transitions in single crystals: A new molecular dynamics method, J Appl Phys. 52 (1981) 7182–7190. https://doi.org/10.1063/1.328693.

[34] T. Darden, D. York, L. Pedersen, Particle mesh Ewald: An N·log(N) method for Ewald sums in large systems, J Chem Phys. 98 (1993) 10089–10092. https://doi.org/10.1063/1.464397.

[35] B. Hess, P-LINCS: A parallel linear constraint solver for molecular simulation, J Chem Theory Comput. 4 (2008) 116–122. https://doi.org/10.1021/ct700200b.

[36] Copyright IBM Corp 1990-2019, Copyright MPI für Festkörperforschung Stuttgart 1997-2001, (n.d.). http://www.cpmd.org/.

[37] R. Car, M. Parrinello, Unified Approach for Molecular Dynamics and Density-Functional Theory, Phys Rev Lett. 55 (1985) 2471–2474.

[38] N. Troullier, J.L. Martins, Efficient pseudopotentials for plane-wave calculations, Phys Rev B. 43 (1991) 1993–2006. https://doi.org/10.1103/PhysRevB.43.1993.

[39] J.P. Perdew, K. Burke, M. Ernzerhof, Generalized gradient approximation made simple, Phys Rev Lett. 77 (1996) 3865.

[40] W. Rudolph, M.H. Brooker, C.C. Pye, Hydration of Lithium Ion in Aqueous Solution, J. Phys. Chem. 99 (1995) 3793–3797. https://pubs.acs.org/sharingguidelines.

[41] M.S. Rodríguez-Barrios, A. Rodríguez-Fortea, L.M. Varela, D. Salavera, M.S. Larrechi, A. Coronas, Structural and quantitative analysis of water association in ethylammonium nitrate mixtures using soft modeling resolution of NIR spectra and molecular dynamics simulations, J Mol Liq. 327 (2021). https://doi.org/10.1016/j.molliq.2020.114789.

[42] J. Workman Jr., L. Weyer, Practical Guide and Spectral Atlas for Interpretive Near-Infrared Spectroscopy, 2nd Edition, CRC Press, Boca Raton, 2012.

[43] D.A. Boryta, Solubility of Lithium Bromide in Water between -50° and +100° C. (45 to 70% Lithium Bromide), J Chem Eng Data. 15 (1961) 142–144.

[44] J.G. Huddleston, A.E. Visser, W.M. Reichert, H.D. Willauer, G.A. Broker, R.D. Rogers, Characterization and comparison of hydrophilic and hydrophobic room temperature ionic liquids incorporating the imidazolium cation, Green Chemistry. 3 (2001) 156–164. https://doi.org/10.1039/b103275p.

[45] T. Méndez-Morales, J. Carrete, Ó. Cabeza, O. Russina, A. Triolo, L.J. Gallego, L.M. Varela, Solvation of lithium salts in protic ionic liquids: A molecular dynamics study, Journal of Physical Chemistry B. 118 (2014) 761–770. https://doi.org/10.1021/jp410090f.

[46] I. Harsányi, L. Pusztai, Hydration structure in concentrated aqueous lithium chloride solutions: A reverse Monte Carlo based combination of molecular dynamics simulations and diffraction data, Journal of Chemical Physics. 137 (2012). https://doi.org/10.1063/1.4767437.

[47] H. Daiguji, E. Hihara, An EXAFS (Extend X-ray Absorption Fine Structure) Study of Aqueous Lithium Bromide Solutions Using Molecular Dynamics Simulation, 1999.

Acknowledgements

The financial support of the Spanish Ministry of Economy and Competitiveness (MAT2017-89239-C2-1-P, MAT2017-89239-C2-2-P and RED2018-102679-T), the Spanish Ministry of Science and Innovation (PID2020-119004RB-C21, PID2021-126148NA-I00 and PID2020-112762GB-I00) and the Xunta de Galicia (GRC ED431C 2020/10) are gratefully acknowledged. MAT and PID2021-126148NA-I00 projects were partially supported by FEDER. Moreover, A.R.P. acknowledges the Spanish Ministry of Education for his FPU grant, T.M.M. acknowledges her contract funded by the pilot program of the USC for the recruitment of distinguished research personnel—call 2021 under the agreement between the USC and the Santander Bank for 2021–2024, and D.L.A. acknowledges to the Diputació de Tarragona and the Universitat Rovira i Virgili for their financial support. Facilities provided by the Galician Supercomputing Centre (CESGA) are also acknowledged.